Version 1.55 as of February 28, 2014
To be submitted to PRL

E06-014 INTERNAL DOCUMENT – NOT FOR PUBLIC DISTRIBUTION

A Precision Measurement of the Neutron Twist-3 Matrix Element d_2: Probing Color Forces

M. Posik,[1,*] D. Flay,[1] D. S. Parno,[2,3] K. Allada,[4] W. Armstrong,[1] T. Averett,[5] F. Benmokhtar,[2] W. Bertozzi,[6] A. Camsonne,[7] M. Canan,[8] G.D. Cates,[9] C. Chen,[10] J.-P. Chen,[7] S. Choi,[11] E. Chudakov,[7] F. Cusanno,[12,13] M. M. Dalton,[9] W. Deconinck,[6] C.W. de Jager,[7] X. Deng,[9] A. Deur,[7] C. Dutta,[4] L. El Fassi,[14] G. B. Franklin,[2] M. Friend,[2] H. Gao,[15] F. Garibaldi,[12] S. Gilad,[6] R. Gilman,[7,14] O. Glamazdin,[16] S. Golge,[8] J. Gomez,[7] L. Guo,[17] O. Hansen,[7] D. W. Higinbotham,[7] T. Holmstrom,[18] J. Huang,[6] C. Hyde,[8,19] H. F. Ibrahim,[20] X. Jiang,[14,17] G. Jin,[9] J. Katich,[5] A. Kelleher,[5] A. Kolarkar,[4] W. Korsch,[4] G. Kumbartzki,[14] J.J. LeRose,[7] R. Lindgren,[9] N. Liyanage,[9] E. Long,[21] A. Lukhanin,[1] V. Mamyan,[2] D. McNulty,[22] Z.-E. Meziani,[1,†] R. Michaels,[7] M. Mihovilovič,[23] B. Moffit,[6,7] N. Muangma,[6] S. Nanda,[7] A. Narayan,[24] V. Nelyubin,[9] B. Norum,[9] Nuruzzaman,[24] Y. Oh,[25] J. C. Peng,[26] X. Qian,[15,27] Y. Qiang,[15,7] A. Rakhman,[28] R. D. Ransome,[14] S. Riordan,[9] A. Saha,[7,‡] B. Sawatzky,[1,7] M. H. Shabestari,[9] A. Shahinyan,[29] S. Širca,[30] P. Solvignon,[31,7] R. Subedi,[9] V. Sulkosky,[6,7] A. Tobias,[9] W. Troth,[18] D. Wang,[9] Y. Wang,[26] B. Wojtsekhowski,[7] X. Yan,[32] H. Yao,[1,5] Y. Ye,[32] Z. Ye,[10] L. Yuan,[10] X. Zhan,[6] Y. Zhang,[33] Y.-W. Zhang,[33,14] B. Zhao,[5] and X. Zheng[9]

(The Jefferson Hall A Collaboration)

[1] *Temple University, Philadelphia, PA 19122*
[2] *Carnegie Mellon University, Pittsburgh, PA 15213*
[3] *Center for Experimental Nuclear Physics and Astrophysics, University of Washington, Seattle, WA 98195*
[4] *University of Kentucky, Lexington, KY 40506*
[5] *College of William and Mary, Williamsburg, VA 23187*
[6] *Massachusetts Institute of Technology, Cambridge, MA 02139*
[7] *Thomas Jefferson National Accelerator Facility, Newport News, VA 23606*
[8] *Old Dominion University, Norfolk, VA 23529*
[9] *University of Virginia, Charlottesville, VA 22904*
[10] *Hampton University, Hampton, VA 23187*
[11] *Seoul National University, Seoul, South Korea*
[12] *INFN, Sezione di Roma, I-00161 Rome, Italy*
[13] *Istituto Superiore di Sanità, I-00161 Rome, Italy*
[14] *Rutgers, The State University of New Jersey, Piscataway, NJ 08855*
[15] *Duke University, Durham, NC 27708*
[16] *Kharkov Institute of Physics and Technology, Kharkov 61108, Ukraine*
[17] *Los Alamos National Laboratory, Los Alamos, NM 87545*
[18] *Longwood University, Farmville, VA 23909*
[19] *Université Blaise Pascal/IN2P3, F-63177 Aubière, France*
[20] *Cairo University, Giza 12613, Egypt*
[21] *Kent State University, Kent, OH 44242*
[22] *University of Massachusetts, Amherst, MA 01003*
[23] *Jožef Stefan Institute, Ljubljana, Slovenia*
[24] *Mississippi State University, MS 39762*
[25] *Kyungpook National University, Taegu 702-701, Republic of Korea*
[26] *University of Illinois at Urbana-Champaign, Urbana, IL 61801*
[27] *Kellogg Radiation Laboratory, California Institute of Technology, Pasadena, Ca 91125*
[28] *Syracuse University, Syracuse, NY 13244*
[29] *Yerevan Physics Institute, Yerevan 375036, Armenia*
[30] *University of Ljubljana, SI-1000 Ljubljana, Slovenia*
[31] *Argonne National Lab, Argonne, IL 60439*
[32] *University of Science and Technology of China, Hefei 230026, People's Republic of China*
[33] *Lanzhou University, Lanzhou 730000, Gansu, People's Republic of China*

(Dated: February 28, 2014)

Double-spin asymmetries and absolute cross-sections were measured at large Bjorken x (which covered the range in x of 0.25 to 0.90), in both the deep inelastic and resonance regions, by scattering longitudinally polarized electrons at beam energies of 4.74 and 5.89 GeV from a transversely and longitudinally polarized ^{3}He target. In this dedicated experiment, the spin structure function g_2 of ^{3}He was determined with precision at large x, and the neutron d_2^n twist-three matrix element was measured at $\langle Q^2 \rangle$ of 3.21 and 4.32 GeV$^2/c^2$, with a precision of about 10^{-5}. Our results are found to be in agreement with Lattice QCD and resolve the disagreement found with previous data at $\langle Q^2 \rangle = 5$ GeV$^2/c^2$. Combining d_2^n and the extracted twist-four matrix element, f_2^n, the average color electric and magnetic forces of the neutron were extracted and found to be of opposite sign and of about 60 MeV/fm in magnitude.

PACS numbers: 12.38.Aw, 12.38.Qk, 13.60.Hb, 13.88.+e, 14.20.Dh

Over the past 30 years, the availability of polarized lepton (electron, muon) beams and targets has enabled an intensive worldwide experimental program of inclusive deep inelastic scattering (DIS) measurements focused on the investigation of the nucleon spin structure [1]. This led to the confirmation of the Bjorken sum rule [2, 3], a fundamental sum rule of quantum chromodynamics (QCD), and the determination of the quarks spin contributions to the total nucleon spin [1]. Exploration of the nucleon spin structure through QCD has shown that both g_1 and g_2 spin structure functions of the nucleon contain contributions from the elusive quark-gluon correlations [4–6] beyond the perturbative-QCD radiative corrections [7–9]. In the case of g_1 these correlations emerge at a higher order in the perturbative expansion in powers of the inverse Q^2 (Q^2 is defined as $-q^2$, where q^2 is the virtual photon probe four-momentum transfer squared) and thus are suppressed, however, they contribute at leading order in g_2. These correlations manifest themselves in $\bar{g}_2$, a deviation of the measured g_2 from the so-called Wandzura-Wilczek value g_2^{WW} [10], which is expressed solely in terms of the g_1 spin structure function:

$$\bar{g}_2(x,Q^2) = g_2(x,Q^2) - g_2^{\mathrm{WW}}(x,Q^2); \quad (1)$$

$$g_2^{\mathrm{WW}}(x,Q^2) = -g_1(x,Q^2) + \int_x^1 g_1(y,Q^2)dy/y, \quad (2)$$

where x is the Bjorken variable interpreted in the infinite momentum frame as being the fraction of longitudinal momentum carried by the leading struck quark in the DIS process. At present there are no *ab initio* calculations of $\bar{g}_2$, nevertheless using the operator product expansion (OPE) [4, 6], the Q^2-dependent quantity

$$d_2 = 3\int_0^1 dx x^2 \bar{g}_2(x) = \int_0^1 dx x^2 \left[3g_2(x) + 2g_1(x)\right] \quad (3)$$

can be related to a specific matrix element containing local operators of quark and gluon fields [11, 12], and is calculable in lattice QCD [13]. Insight into the physical meaning of d_2 was articulated by Ji [14] who expressed d_2 in terms of a linear combination of χ_E and χ_B, dubbed the electric and magnetic "color polarizabilities", summed over the quarks flavors.

$$\chi_E \vec{S} = \frac{1}{2M^2}\langle P,S|q^\dagger \vec{\alpha} \times g\vec{E}q|P,S\rangle, \quad (4)$$

$$\chi_B \vec{S} = \frac{1}{2M^2}\langle P,S|q^\dagger g\vec{B}q|P,S\rangle, \quad (5)$$

where P and S are the nucleon momentum and spin, q and $q^\dagger$ are the quark fields, $\vec{E}$ and $\vec{B}$ the average color electric and magnetic fields seen by the struck quark, $\vec{\alpha}$ the velocity of the struck quark, g is the strong coupling parameter, and M is the nucleon mass.

More recently Burkardt [15] identified d_2 as being proportional to the instantaneous average sum of the transverse electric $F_E^y(0)$ and magnetic $F_B^y(0)$ color forces the struck quark experiences at the instant it is hit by the virtual photon due to the remnant di-quark system in the DIS process. The net average force contributes in part to what is called the "chromodynamic lensing" effect in semi-inclusive DIS where the struck quark experiences color forces as it exits the nucleon before converting into an outbound hadron [15, 16]. The relations between the color forces, the color polarizabilities and the matrix elements of the quark-gluon correlations are given by:

$$F_E^y(0) = -\frac{M^2}{4}\chi_E = -\frac{M^2}{4}\left[\frac{2}{3}(2d_2 + f_2)\right], \quad (6)$$

$$F_B^y(0) = -\frac{M^2}{2}\chi_B = -\frac{M^2}{2}\left[\frac{1}{3}(4d_2 - f_2)\right], \quad (7)$$

where f_2 is a twist-4 quark-gluon correlations matrix element related to the x^2 moment of the g_3 spin structure function. The twist-4 matrix element has never been directly measured but may be extracted by taking advantage of the Q^2 dependence of $g_1(x,Q^2)$ [17, 18], since it appears as a higher order contribution suppressed by $1/Q^2$ in the first moment of g_1: $\Gamma_1 = \int_0^1 dx g_1(x,Q^2)$.

The neutron d_2 (d_2^n) has been calculated in different nucleon structure models [19–21] and in lattice QCD [13]. The results consistently give a small negative value deviating from the world measured positive value by about 2 standard deviations [22, 23]. At a fundamental level the forces d_2 probes are in part responsible for the "confinement" of constituents, measuring them and understanding them in QCD is an important goal. The significant discrepancy between the measurement and the theory results of d_2^n called for a dedicated measurement to explore this issue.

The E06-014 experiment [24] was performed at Jefferson Lab (JLab) in Hall A [25] from February to March of 2009. In this experiment measurements of inclusive scattering of a longitudinally polarized electron beam off a polarized ^{3}He target were carried out at two incident beam energies of 4.74 GeV and 5.89 GeV and with two states of target polarization, transverse (perpendicular to the electron beam in the scattering plane) and longitudinal (along the electron beam). Scattered electrons with momenta ranging from 0.7 to 2 GeV/c were detected in both the BigBite spectrometer (BBS) [26] and the left high resolution spectrometer (LHRS) [25] each set at a scattering angle of 45°. The large momentum and angular acceptance (~ 64 msr) of the BBS allowed it to precisely measure the double-spin asymmetries (DSA) over the full momentum range at one current setting of the spectrometer. The absolute cross sections were obtained from the well understood LHRS by scanning over the same momentum range in discrete steps. The longitudinal (transverse) DSA is defined as

$$A_{\parallel(\perp)} = \frac{1}{P_t P_b D_{\mathrm{N}_2}} \frac{1}{(\cos\phi)} \frac{N^{\downarrow\Uparrow(\Rightarrow)} - N^{\uparrow\Uparrow(\Rightarrow)}}{N^{\downarrow\Uparrow(\Rightarrow)} + N^{\uparrow\Uparrow(\Rightarrow)}}, \quad (8)$$

where N is the number of electrons, P_t is the target polarization, P_b is the electron polarization, D_{N_2} is the nitrogen dilution factor to account for the small amount ($\sim 1\%$ of ^{3}He density) of N_2 present in the ^{3}He target to reduce depolarization effects, ϕ is the vertical scattering angle (with $\cos\phi$ applied only to the transverse asymmetry). The single arrows refer to the electron helicity direction and the double arrows refer to the target spin direction. The orientation of the latter are such that arrows pointing to the right (left) represent spins that are transverse to the electron momentum while arrows pointing up (down) represent spins parallel (anti-parallel) to the electron momentum.

The incident electron beam polarization was measured using two independent polarimeters based on Møller [27] and Compton [28, 29] scattering, whose combined analysis yielded an average electron-beam polarization of 71.87% ± 1.13% [30]. The residual beam-charge asymmetry was controlled to within 100 ppm through the use of a feedback loop.

The scattered electrons interacted with about 8 atms of polarized ^{3}He gas contained in a 40 cm long target cell. The ^{3}He nuclei were polarized via double spin-exchange optical pumping of a Rb-K mixture [31]. Nuclear magnetic resonance (NMR) measurements were taken approximately every 4 hours to monitor the target polarization. The relative NMR measurements were calibrated with absolute electron paramagnetic resonance measurements, which were taken every few days. Additionally, the longitudinal target polarization was cross-checked using water NMR measurements. The average target polarization achieved was 50.5% ± 3.6%.

The BBS consisted of a large-aperture dipole magnet in front of a detector stack whose configuration was similar to that found in reference [32], with an addition of a newly installed threshold gas Čerenkov detector [33], which was used for pion rejection. The optics software package used for the BBS was calibrated at an incident energy of 1.2 GeV using various targets described in reference [32]. Angular and momentum resolutions of 10 mrad and 1% were achieved [30, 33]. To keep trigger rates compatible with a high live time of the data acquisition ($\gtrsim 80\%$), the main electron trigger was formed from a geometrical overlap between the shower calorimeter layers and Čerenkov signals. The BBS achieved a total pion rejection factor that was better than 10^4.

The LHRS is a small acceptance spectrometer (~ 6 msr) and was used with its standard detector package of two vertical drift chambers used for charged-particle tracking, two scintillator planes used for triggering and timing of charged particles, a light gas Čerenkov counter, and a lead-glass calorimeter used for electron identification. Optics calibrations [32] for the LHRS used the same targets that were used to calibrate the BigBite optics. The LHRS achieved a pion rejection factor better than 10^5, and measured the e^-–^{3}He inclusive cross section to better than 8%.

The two main sources of background contamination of the electron sample were charged pions and pair-produced electrons resulting from the conversion of π^0 decay photons. The BBS π^- (π^+) contamination of the e^- (e^+) sample was estimated from the pre-shower energy spectrum and found to be less than 3% (6.5%) across the momentum acceptance for π^- (π^+). Weighting the measured $\pi^\pm$ asymmetries by the pion contamination resulted in a negligible asymmetry contamination of the electron DSA. The $\pi^\pm$ contamination measured in the LHRS was negligible.

Assuming symmetry between the pair-produced electrons and positrons, the electron background was directly measured by reversing the BBS and LHRS magnet polarities resulting in positrons, rather than electrons, being steered into the detectors. By switching the magnet polarity both electrons and positrons see the same acceptance which then drops out when forming the e^+/e^- ratio . The positron cross section was measured with the LHRS and subtracted from the electron cross section. We used the BBS measured and fitted e^+/e^- ratios, along with statistically weighted positron asymmetry measurements, to determine the amount of pair-production contamination in the electron sample. The e^+/e^- ratio at low-x ($\langle x \rangle = 0.275$) was about 56%, and quickly fell off to below 1% as x increased. The positron asymmetry was measured with the BBS magnet in normal polarity to be about 1-2%. The positron asymmetries were cross checked by reversing the BBS magnet polarity and measuring the positron asymmetry for one DSA setting. The background and false asymmetries were removed from the electron asymmetries as shown in Eq. 9, where c_1 is the π^-/e^- ratio; c_2 is the π^+/e^+ ratio; c_3 is the e^+/e^- ratio; $A^{m(e^+)}_{\perp,\parallel}$ is the measured electron (positron) asymmetry defined in Eq. 8.

$$A^{e^-}_{\perp,\parallel} = \frac{A^m_{\perp,\parallel} - c_3 A^{e+}_{\perp,\parallel}}{1 - c_1 - c_3 + c_2 c_3}. \quad (9)$$

Lastly, the electromagnetic internal and external radiative corrections were performed on the unpolarized cross section σ_0 using the formalism of Mo and Tsai [34, 35]. The elastic [34] and quasi-elastic [36] radiative tails were subtracted using form factors from [37] and [38]. The inelastic corrections were evaluated using the F1F209 model [39] for the unmeasured cross sections in the resonance and DIS regions. We followed the formalism of Akushevich *et al.* [40] to perform the radiative corrections on $\Delta\sigma_{\parallel,\perp} = 2\sigma_0 A_{\parallel,\perp}$, the polarized cross-section differences. Here, the exact elastic polarized cross-section difference tails were found to be negligible. The remaining quasi-elastic [41, 42], resonance [43], and deep inelastic regions [44] were treated together using inputs from their respective models. The size of the total corrections in all cases did not exceed 45% of the measured σ_0, $\Delta\sigma_\parallel$, and $\Delta\sigma_\perp$. While the magnitude of this correction is significant, the associated absolute uncertainty on the radiative corrections on g_1 and g_2 were less than 5%, which is smaller than their statistical uncertainty.

We show in Fig. 1 the x^2 weighted polarized spin structure function g_2 on ^{3}He, formed from the measured Born asymmetries and cross sections according to

$$g_2^{^3\text{He}} = \frac{MQ^2}{4\alpha^2}\frac{y^2\sigma_0}{(1-y)\,(2-y)} \times \left[-A_\parallel^{e^-} + \frac{1+(1-y)\cos\theta}{(1-y)\sin\theta}A_\perp^{e^-}\right], \quad (10)$$

where σ_0 is the ^{3}He Born cross section, α the electromagnetic coupling constant, $y = E - E'/E$ the fraction of the incident electron energy lost in the nucleon rest frame and θ the electron scattering angle. Note the dramatic improvement of the statistical precision of our data in Figure 1a compared to the existing world data at large $x \geq 0.3$. For clarity, Figure 1b is zoomed in by a factor of 10 and shows only a subset of the world data.

The measured DSAs and cross sections at each beam energy were used to evaluate $d_2^{^3\text{He}}$ at two mean $< Q^2 >$ values (3.21 and 4.32 GeV$^2/c^2$) according to

$$d_2^{^3\text{He}} = \int_{0.25}^{0.90} dx \frac{MQ^2}{4\alpha^2}\frac{x^2y^2\sigma_0}{(1-y)\,(2-y)} \times \left[\left(3\frac{1+(1-y)\cos\theta}{(1-y)\sin\theta} + \frac{4}{y}\tan\frac{\theta}{2}\right)A_\perp^{e^-} + \left(\frac{4}{y}-3\right)A_\parallel^{e^-}\right]. \quad (11)$$

The upper integration limit of $x = 0.90$ was chosen in order to avoid the quasi-elastic peak and the Δ resonance. In addition to using Eq. 11, the Nachtmann moments [45] may be used to evaluate $d_2^{^3\text{He}}$, but the difference between the two approaches at our kinematics is smaller than the statistical precision of our measured $d_2^{^3\text{He}}$ value. Neutron information was extracted from $d_2^{^3\text{He}}$ through the expression

$$d_2^n = \frac{d_2^{^3\text{He}} - (2P_p - 0.014)\,d_2^p}{P_n + 0.056}, \quad (12)$$

where P_p and P_n are the effective proton and neutron polarizations in ^{3}He, and the factors 0.056 and 0.014 are due to the Δ-isobar contributions [46]. d_2^p in Eq. 12, was calculated from various global analyses [44, 47–51] to be (-17.5±5.3)$\times 10^{-4}$ and (-16.9±4.7)$\times 10^{-4}$ at the kinematics of E06-014 at average $\langle Q^2 \rangle$ values of 3.23 and 4.32 GeV$^2/c^2$, respectively.

The d_2^n values measured during E06-014 represent only partial integrals. The full integrals can be evaluated by computing the low- and high-x contributions. The low-x contribution is suppressed due to the x^2-weighting of the d_2 integrand, and was calculated by fitting existing g_1^n [52–55] and g_2^n [22, 53, 56] data. The fits to both structure functions were dominated by the precision data from Ref. [53], and extended in x from 0.02 to 0.25. Possible Q^2 dependence of this low-x contribution was presumed to be negligible in this analysis. The high-x contribution, dominated by the elastic x =1 contribution with a negligible contribution from 0.9 to $x < 1$, was estimated using the elastic form factors G_E^n and G_M^n, computed from the

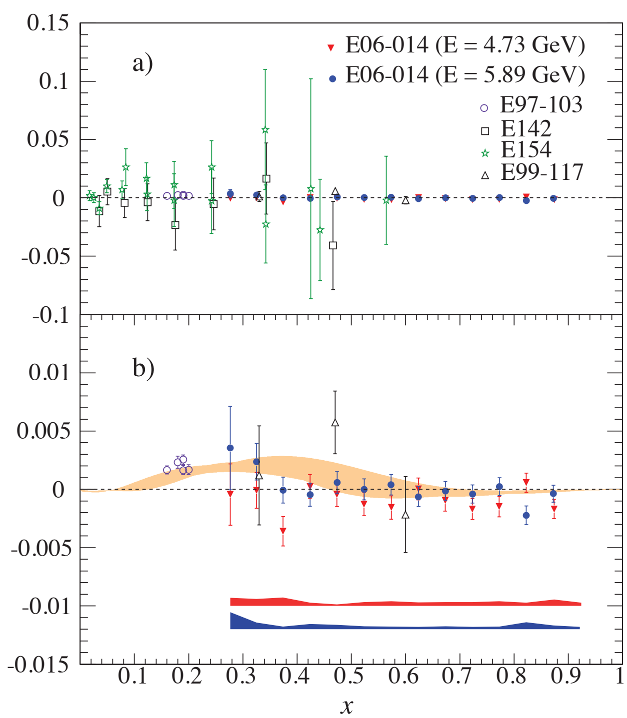

FIG. 1. x^2 weighted $g_2^{^3\text{He}}$ plotted against x. Panel a) illustrates the increased precision of our results compared to the world data [23, 52, 53, 55]. All error bars on the world data are statistical and systematic uncertainties added in quadrature. Panel b) is zoomed by a factor of 10 in the vertical scale and displays only a subset of the world data. The error bars on the E06-014 data are statistical only. The top (red) and bottom (blue) bands represent the systematic uncertainty associated with the E = 4.74 and 5.89 GeV data sets, respectively. The yellow band shows the $g_2^{\text{WW},^3\text{He}}$ coverage from several global analyses [44, 47–51].

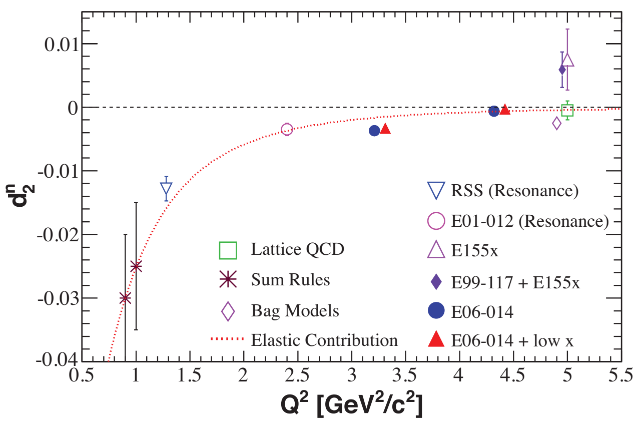

FIG. 2. World d_2^n data [22, 23, 56, 58, 59], model predictions from lattice QCD [13], QCD sum rules [19, 20], a and bag model [21], along with the results of E06-014 are plotted against Q^2 (all data includes the elastic contribution). The E06-014 measured d_2^n without (with) the low-x contributions added are represented by blue solid circle (solid red up triangle) markers, and are offset in Q^2 for clarity. The inner error bar ticks on the E06-014 results represent the systematic uncertainty, while the outer error bar ticks represent the statistical uncertainties. The world data error bars represent the in quadrature sum of the statistical and systematic uncertainties.

Galster parameterization [57] and dipole model, respectively. The individual contributions used to evaluate the full d_2^n integral are listed in Table I.

The fully integrated d_2^n results from this experiment are shown as a function of Q^2 in Fig. 2 along with the world data and available calculations. We find that our d_2^n results are in agreement with the lattice QCD [13] and bag model [21] calculations, which predict a small negative value of d_2^n at large Q^2. We note that at lower Q^2 the elastic contribution of d_2^n dominates the measured values and is in agreement with the QCD sum rule calculations [19, 20]. Given the precision of our measurements, we find a much smaller d_2^n value than that reported by the SLAC E155 experiment.

Primed with a new value of d_2^n, we proceeded to determine f_2^n and extract the average electric and magnetic color forces. f_2^n was extracted following the analysis described in [17, 33] but with updated a_2^n matrix elements evaluated from global analyses [44, 47–51], which were found to be $(5.7\pm12.0)\times10^{-4}$ at $\langle Q^2\rangle = 3.21$ GeV$^2/c^2$ and $(1.5\pm11.0)\times10^{-4}$ at $\langle Q^2\rangle = 4.32$ GeV$^2/c^2$, updated d_2^n (Table I) values, and the inclusion of the Γ_1 datum from JLab RSS experiment [59]. The singlet axial charge, $\Delta\Sigma$, was determined from values of Γ_1^n at $Q^2 \geq 5$ GeV$^2/c^2$ to be 0.375 ± 0.052, in excellent agreement with that found in [60]. A summary of our f_2^n and average color force values, along with calculations from several models, can be found in Table II.

In summary, we have measured the DSA and absolute cross sections from a polarized ^{3}He target, allowing for the precision measurement of the neutron d_2. We find that d_2^n is in general small, and negative at $\langle Q^2\rangle = 3.21$ GeV$^2/c^2$, and consistent with zero at $\langle Q^2\rangle = 4.32$ GeV$^2/c^2$. In contrast with previous results we find values consistent with the lattice QCD [13] and bag [21] predictions. We used our d_2^n measurements to extract the twist-4 matrix element f_2^n and performed a decomposition into neutron average electric and magnetic color forces. Our results show that f_2^n is much larger then d_2^n, implying the neutron electric and magnetic color forces are nearly equal in magnitude but opposite in sign.

We would like to thank the JLab Hall A technical staff and Accelerator Division for their outstanding support, as well as M. Burkardt, L. P. Gamberg, W. Melnitchouk, A. Metz, and J. Soffer for their useful discussions. One of us (Z.-E.M.) would like to particularly thank X. Ji for his encouragements to propose and perform this measurement since 1995. This work was supported in part by DOE grants DE-FG02-87ER40315 and DE-FG02-94ER40844 (from Temple University). Jefferson Lab is operated by the Jefferson Science Associates, LLC, under DOE grant DE-AC05-060R23177.

* mposik1983@gmail.com
† meziani@temple.edu
‡ Deceased

[1] C. A. Aidala, S. D. Bass, D. Hasch and G. K. Mallot, Rev. Mod. Phys. **85**, 655 (2013), and references therein.
[2] J. D. Bjorken, Phys. Rev. **148**, 1467 (1966).
[3] J. D. Bjorken, Phys. Rev. D **1**, 1376 (1970).
[4] E. V. Shuryak and A. I. Vainshtein, Nucl. Phys. B **201**, 141 (1982).
[5] R. L. Jaffe, Comments Nucl. Part. Phys. **19**, 239 (1990).
[6] R. L. Jaffe and X. -D. Ji, Phys. Rev. D **43**, 724 (1991).
[7] V. N. Gribov and L. N. Lipatov, Sov. J. Nucl. Phys. **15**, 438 (1972) [Yad. Fiz. **15**, 781 (1972)].
[8] G. Altarelli and G. Parisi, Nucl. Phys. B **126**, 298 (1977).
[9] Yu. L. Dokshitzer, Sov. Phys. JETP **46**, 641(1977).
[10] S. Wandzura and F. Wilczek, Phys. Lett. B **72**, 195 (1977).
[11] X. -D. Ji and P. Unrau, Phys. Lett. B **333**, 228 (1994).
[12] E. Stein, P. Gornicki, L. Mankiewicz and A. Schafer, Phys. Lett. B **353**, 107 (1995).
[13] M. Gockeler, R. Horsley, D. Pleiter, P. E. L. Rakow, A. Schafer, G. Schierholz, H. Stuben and J. M. Zanotti, Phys. Rev. D **72**, 054507 (2005).
[14] X. -D. Ji, In *Santa Fe 1995, Baryons '95* 25-34 [hep-ph/9510362].
[15] M. Burkardt, Phys. Rev. D **88**, 114502 (2013).
[16] M. Burkardt, Nucl. Phys. A **735**, 185 (2004).
[17] Z. -E. Meziani, W. Melnitchouk, J. -P. Chen, S. Choi, T. Averett, G. Cates, C. W. de Jager and A. Deur *et al.*, Phys. Lett. B **613**, 148 (2005).
[18] M. Osipenko, W. Melnitchouk, S. Simula, P. E. Bosted, V. Burkert, M. E. Christy, K. Griffioen and C. Keppel *et*

TABLE I. Our measured d_2^n, along with the low-x and elastic d_2^n contributions, which were used in evaluating the full d_2^n integrals.

$\langle Q^2 \rangle$ (GeV^2/c^2)	Measured ($\times 10^{-5}$)	Low x ($\times 10^{-5}$)	Elastic ($\times 10^{-5}$)	Total d_2^n ($\times 10^{-5}$)
3.21	-261.0 $\pm$ 79.0$_{\mathrm{stat}}$ $\pm$ 48.0$_{\mathrm{sys}}$	38.0 $\pm$ 58.0	-108.0	-331.0 $\pm$ 79.0$_{\mathrm{stat}}$ $\pm$ 75.0$_{\mathrm{sys}}$
4.32	4.0 $\pm$ 83.0$_{\mathrm{stat}}$ $\pm$ 37.0$_{\mathrm{sys}}$	38.0 $\pm$ 58.0	-69.0	-27.0 $\pm$ 83.0$_{\mathrm{stat}}$ $\pm$ 69.0$_{\mathrm{sys}}$

TABLE II. Our results for f_2^n, F_E and F_B compared to model calculations. The value for d_2^n is assumed to be zero in the Instanton model calculation, as it is much smaller than f_2^n [61].

Group	Q^2 (GeV^2/c^2)	$f_2^n \times 10^{-3}$	F_E (MeV/fm)	F_B (MeV/fm)
E06-014	3.21	76.23 $\pm$ 0.79 $\pm$ 40.1	-51.85 $\pm$ 1.32 $\pm$ 29.90	66.64 $\pm$ 2.43 $\pm$ 30.00
E06-014	4.32	73.29 $\pm$ 0.83 $\pm$ 40.1	-54.18 $\pm$ 1.37 $\pm$ 29.90	55.39 $\pm$ 2.53 $\pm$ 30.00
Instanton [61, 62]	0.40	38.0	-30.41	30.41
QCD sum rule [12, 19]	1	-13.0 $\pm$ 6.0	54.25 $\pm$ 15.52	79.52 $\pm$ 30.06
QCD sum rule [20]	1	10.0 $\pm$ 10.0	29.73 $\pm$ 16.62	81.75 $\pm$ 30.64

al., Phys. Lett. B **609**, 259 (2005).
[19] E. Stein, P. Gornicki, L. Mankiewicz, A. Schafer and W. Greiner, Phys. Lett. B **343**, 369 (1995).
[20] I. I. Balitsky, V. M. Braun and A. V. Kolesnichenko, Phys. Lett. B **242**, 245 (1990) [Erratum-ibid. B **318**, 648 (1993)].
[21] X. Song, Phys. Rev. D **54**, 1955 (1996).
[22] P. L. Anthony *et al.* [E155 Collaboration], Phys. Lett. B **553**, 18 (2003).
[23] X. Zheng *et al.* [Jefferson Lab Hall A Collaboration], Phys. Rev. C **70**, 065207 (2004).
[24] S. Choi, X. Jiang, Z.-E. Meziani, B. Sawatzky, spokespersons, Jefferson Lab Experiment E06-014, `http://www.jlab.org/exp_prog/proposals/06/PR06-014.pdf`.
[25] J. Alcorn, B. D. Anderson, K. A. Aniol, J. R. M. Annand, L. Auerbach, J. Arrington, T. Averett and F. T. Baker *et al.*, Nucl. Instrum. Meth. A **522**, 294 (2004).
[26] D. J. J. de Lange, J. J. M. Steijger, H. de Vries, M. Anghinolfi, M. Taiuti, D. W. Higinbotham, B. E. Norum and E. Konstantinov, Nucl. Instrum. Meth. A **406**, 182 (1998).
[27] A. V. Glamazdin, V. G. Gorbenko, L. G. Levchuk, R. I. Pomatsalyuk, A. L. Rubashkin, P. V. Sorokin, D. S. Dale and B. Doyle *et al.*, Fizika B **8**, 91 (1999).
[28] S. Escoffier, P. Y. Bertin, M. Brossard, E. Burtin, C. Cavata, N. Colombel, C. W. de Jager and A. Delbart *et al.*, Nucl. Instrum. Meth. A **551**, 563 (2005).
[29] M. Friend, D. Parno, F. Benmokhtar, A. Camsonne, M. Dalton, G. B. Franklin, V. Mamyan and R. Michaels *et al.*, Nucl. Instrum. Meth. A **676**, 96 (2012).
[30] D. Parno, Ph.D. thesis, Carnegie Mellon University, `http://hallaweb.jlab.org/experiment/E06-014/talks/DianaParno_Dissertation.pdf`(2011).
[31] E. Babcock, I. Nelson, S. Kadlecek, B. Driehuys, L. W. Anderson, F. W. Hersman and T. G. Walker, Phys. Rev. Lett. **91**, 123003 (2003).
[32] X. Qian *et al.* [Jefferson Lab Hall A Collaboration], Phys. Rev. Lett. **107**, 072003 (2011).
[33] M. Posik, Ph.D. thesis, Temple University, `http://hallaweb.jlab.org/experiment/E06-014/talks/posik_dissertation.pdf` (2014).
[34] L. W. Mo and Y. -S. Tsai, Rev. Mod. Phys. **41**, 205 (1969).
[35] Y. -S. Tsai, SLAC-PUB-0848.
[36] S. Stein, W. B. Atwood, E. D. Bloom, R. L. Cottrell, H. C. DeStaebler, C. L. Jordan, H. Piel and C. Y. Prescott *et al.*, Phys. Rev. D **12**, 1884 (1975).
[37] A. Amroun, V. Breton, J. M. Cavedon, B. Frois, D. Goutte, F. P. Juster, P. Leconte and J. Martino *et al.*, Nucl. Phys. A **579**, 596 (1994).
[38] J. W. Lightbody and J. S. O'Connell, Comp. in. Phys. **2(3)**, 57 (1988).
[39] P. E. Bosted and V. Mamyan, arXiv:1203.2262 [nucl-th].
[40] I. Akushevich, A. Ilyichev, N. Shumeiko, A. Soroko and A. Tolkachev, Comput. Phys. Commun. **104**, 201 (1997).
[41] P. E. Bosted, Phys. Rev. C **51**, 409 (1995).
[42] J. E. Amaro, M. B. Barbaro, J. A. Caballero, T. W. Donnelly, A. Molinari and I. Sick, Phys. Rev. C **71**, 015501 (2005).
[43] D. Drechsel, S. S. Kamalov and L. Tiator, Eur. Phys. J. A **34**, 69 (2007).
[44] D. de Florian, R. Sassot, M. Stratmann and W. Vogelsang, Phys. Rev. Lett. **101**, 072001 (2008).
[45] O. Nachtmann, Nucl. Phys. B **63**, 237 (1973).
[46] F. R. P. Bissey, V. A. Guzey, M. Strikman and A. W. Thomas, Phys. Rev. C **65**, 064317 (2002).
[47] D. de Florian, G. A. Navarro and R. Sassot, Phys. Rev. D **71**, 094018 (2005).
[48] C. Bourrely, J. Soffer and F. Buccella, Eur. Phys. J. C **23**, 487 (2002).
[49] C. Bourrely, J. Soffer and F. Buccella, Phys. Lett. B **648**, 39 (2007).
[50] E. Leader, A. V. Sidorov and D. B. Stamenov, Phys. Rev. D **73**, 034023 (2006).
[51] T. Gehrmann and W. J. Stirling, Phys. Rev. D **53**, 6100 (1996).
[52] P. L. Anthony *et al.* [E142 Collaboration], Phys. Rev. D **54**, 6620 (1996).
[53] K. Kramer, D. S. Armstrong, T. D. Averett, W. Bertozzi, S. Binet, C. Butuceanu, A. Camsonne and G. D. Cates *et al.*, Phys. Rev. Lett. **95**, 142002 (2005).
[54] K. Abe *et al.* [E143 Collaboration], Phys. Rev. D **58**, 112003 (1998).
[55] K. Abe *et al.* [E154 Collaboration], Phys. Lett. B **404**,

377 (1997).
[56] P. L. Anthony *et al.* [E155 Collaboration], Phys. Lett. B **458**, 529 (1999).
[57] S. Galster, H. Klein, J. Moritz, K. H. Schmidt, D. Wegener and J. Bleckwenn, Nucl. Phys. B **32**, 221 (1971).
[58] P. Solvignon *et al.* [E01-012 Collaboration], arXiv:1304.4497 [nucl-ex].
[59] K. Slifer *et al.* [RSS Collaboration], Phys. Rev. Lett. **105**, 101601 (2010).
[60] A. Accardi, J. L. Albacete, M. Anselmino, N. Armesto, E. C. Aschenauer, A. Bacchetta, D. Boer and W. Brooks *et al.*, arXiv:1212.1701 [nucl-ex].
[61] J. Balla, M. V. Polyakov and C. Weiss, Nucl. Phys. B **510**, 327 (1998).
[62] N. -Y. Lee, K. Goeke and C. Weiss, Phys. Rev. D **65**, 054008 (2002).